Evolution of dry patches in evaporating liquid films

Vladimir S. Ajaev
Department of Mathematics, Southern Methodist University, Dallas, Texas 75275, USA
(Received 26 January 2005; published 19 September 2005)

We investigate evolution of dry patches in a thin film of a volatile liquid on a heated plate in the framework of a model that accounts for the effects of surface tension, evaporation, thermocapillarity, and disjoining pressure. Dry areas on the plate are modeled by isothermal microscopic films which are in thermodynamic equilibrium with the vapor. For nonpolar liquids such equilibrium is achieved due to van der Waals forces, well-defined capillary ridges are formed around growing dry patches, contact line speed increases with time. For polar liquids the microscopic film is formed by combined action of van der Waals and electrical double layer forces, capillary ridge is small, and contact line speed quickly approaches a constant value. Thermocapillary stresses tend to increase the height of the capillary ridges formed around expanding patches. Numerical simulations demonstrate that the proposed model is capable of describing a number of complicated phenomena observed in experimental studies of evaporating films including fingering instabilities and merger of growing dry patches.

DOI: 10.1103/PhysRevE.72.031605 PACS number(s): 68.15.+e, 47.54.+r

I. INTRODUCTION

Moving contact lines in air-liquid-solid systems have been studied extensively [1,2]. A variety of insteresting phenomena, such as contact angle hysteresis, fingering instability, and formation of various dewetting patterns, has been observed experimentally and explained theoretically. However, a related problem of motion of a line of contact between solid, liquid, and vapor phase of the same liquid, received much less attention. Experimental investigations of such moving contact lines have been carried out only recently and uncovered remarkably rich dynamics in a simple problem of nucleation and growth of dry patches in thin liquid films [3]. Initially circular dry patches became unstable as they expanded, resulting in formation of fingers, i.e., liquid rivulets protruding towards the dry region. Related experiments on laser melting of thin metal films [4] demonstrated that dynamics of dewetting in evaporating liquid films with a large number of dry patches is similar to dynamics of spinodal decomposition in mixtures.

Several theoretical investigations of dewetting in thin evaporating films [5–8] suggest that dynamics of dry patches in polar liquids is determined by the interplay between long-range van der Waals forces and short-range contributions to the disjoining pressure from the electrical double layers. Schwartz *et al.* [7] accounted for both contributions in their two-dimensional simulations of thin films of volatile liquids in the framework of a simplified evaporation model. Lyushnin *et al.* [8] studied stability of growing dry patches in liquid films in the framework of a more elaborate evaporation model but they did not consider the effects of heat transfer in the film and thermocapillary stresses at the vapor-liquid interface. We also note that most mathematical models [5,8] are limited to ultrathin films (of thickness $\sim$10 nm), while experimental studies often involve films which are thicker by orders of magnitude.

Significant progress in understanding the effects of evaporation and heat transfer on viscous flow near a contact line has been made in several studies of steady menisci in contact with heated surfaces [9–12]. Dry areas on heated surfaces are modeled in these studies by microscopic adsorbed films which are in thermodynamic equilibrium with both solid and vapor phases due to van der Waals forces. The contact line is then defined as the region of rapid change of interfacial curvature, i.e., the front between "wet" and "dry" parts of the substrate. While originally developed for steady contact lines [9–12], this approach has been incorporated into models of unsteady viscous flows as well, e.g., in a recent study of axisymmetric spreading of volatile droplets on heated surfaces [13].

In the present study we describe coupled liquid flow and heat transfer in evaporating films using the general framework of the previous studies [9–13], but our model of disjoining pressure accounts for contributions from both van der Waals forces and electrical double layers. The latter is significant for polar liquids, such as water, on most substrates. The effects of disjoining pressure, thermocapillary stresses, and evaporation intensity on an isolated growing dry patch are investigated. Furthermore, the mathematical model of contact lines based on the works of Potash and Wayner [9] and Moosman and Homsy [10] is incorporated into numerical simulations of evolution of complicated two-dimensional vapor-liquid interfaces. These numerical simulations allow us to investigate fingering instability and interaction of growing dry patches in evaporating liquid films.

II. FORMULATION

We consider a thin film of a volatile liquid of density ρ and viscosity μ on a heated rigid plate. The standard one-sided model of evaporation [14] allows us to neglect all dynamical processes in the vapor. The plate temperature is elevated above the equilibrium saturation temperature at the vapor pressure T_S^*; the latter is used as the temperature scale. We use the capillary scale $C^{1/3}\sigma_0/R$ for the pressure, where σ_0 is the surface tension at the temperature T_S^*, R is the characteristic length in the horizontal direction, also used as the

length scale. The velocity scale U is determined from the interfacial mass balance as described in Ref. [12]:

$$U = \frac{kT_S^*}{\rho \mathcal{L} R},$$

where $\mathcal{L}$ is the latent heat of vaporization and k is the thermal conductivity of the liquid. We define the capillary number as $C = \mu U/\sigma_0$ and develop our mathematical model based on the assumption that the capillary number is a small parameter.

Formulation of the governing equations and boundary conditions for viscous flow and heat transfer in the film is straightforward [12,15] and therefore is not repeated here. The only aspect of the formulation that has to be discussed in more detail is the relationship between the mass flux and local temperature at the interface. Two phases are in equilibrium at the saturation temperature T_S^* when pressures in both phases are equal. In evaporating films considered in the present study there is a pressure jump across the liquid-vapor interface due to capillarity and disjoining pressure. This pressure jump and the evaporative mass flux across the interface J (scaled by $\rho U C^{1/3}$) are the factors that affect the local interfacial temperature. Assuming that corrections from each are small, we can use the following nondimensional linearized expression for T^i, the difference between the interfacial and saturation temperatures scaled by $C^{2/3}T_S^*$:

$$T^i = KJ - \delta(p - p_v),$$

$$K = \frac{\rho U}{2\rho_v \mathcal{L} C^{1/3}} \sqrt{2\pi \bar{R} T_S^*}, \quad \delta = \frac{\sigma_0}{\mathcal{L}\rho R C^{1/3}}. \tag{1}$$

This condition has been derived based on kinetic gas theory [9,10], the parameters K and δ characterize the effects of evaporation kinetics and the pressure jump across the interface on the local value of T^i; ρ_v is the vapor density, $\bar{R}$ is the gas constant per unit mass.

A lubrication-type approach for steady evaporating films on heated surfaces has been formulated in Ref. [12] based on the assumption that the film thickness scales as $C^{1/3}R$. This approach can be extended to unsteady thin film flows, as was shown in the context of spreading of thin volatile droplets on heated surfaces [13]. The two-dimensional version of the evolution equation for film thickness h derived in Ref. [13] can be written in the form

$$h_t - \frac{\delta(\nabla^2 h + \Pi) - T_0}{K + h} + \frac{1}{3}\nabla\left[h^3 \nabla(\nabla^2 h + \Pi)\right] - \frac{M}{2}\nabla \cdot \left[h^2 \nabla\left(T_0 - \frac{T_0 - \delta(\nabla^2 h + \Pi)}{Kh^{-1} + 1}\right)\right] = 0, \tag{2}$$

where T_0 is the scaled temperature of the heated rigid plate, Π is the disjoining pressure specified below, derivatives are taken with respect to Cartesian coordinates x and y; both axes are directed along the heated plate.

The second term on the left hand side of Eq. (2) is responsible for evaporative mass losses, the third term is due to viscous flow driven by a combination of capillary and disjoining pressure gradients, and the fourth term is a contribution from the Marangoni stresses. The modified Marangoni number is defined by

$$M = \frac{T_S^*}{\sigma_0}\left|\frac{d\sigma}{dT}\right|,$$

the surface tension is assumed to be a decreasing linear function of temperature. Equation (2) is the key equation in our analysis. Once it is solved for the film thickness $h(x,y,t)$ all other field variables are known.

Since many important dry-out experiments are carried out for polar liquids, e.g., water on mica surface [3], we use the appropriate expression for the disjoining pressure in the form

$$\Pi = S\exp(-\xi h) + \varepsilon/h^3. \tag{3}$$

This formula allows us to describe uniform microscopic films formed by the combined action of long-range and short-range forces. The latter are characterized by a nondimensional parameter $S = S^P e^{d_0/l_0}(R/\sigma_0 l_0)$ (S^P is the polar component of the spreading coefficient, d_0 is the molecular interaction distance, and l_0 is the Debye length), ξ is the ratio of the initial film thickness and the Debye length, and ε is the scaled Hamaker constant [$\varepsilon = |A|/(\sigma_0 R^2 C)$]. The case of nonpolar liquids considered in Refs. [12,13] can be easily recovered by taking $S = 0$.

III. CONTACT LINE SPEED

Shapes of dry patches observed in experiments with evaporating films are often quite complicated, but the basic physical effects contributing to their evolution can be understood using the one-dimensional version of Eq. (2). In this section, we assume that the film thickness is a function of x and t only and solve the evolution equation numerically on an interval $[0,L]$ for constant T_0 using a finite-difference approach. BDF method from the standard DVODE solver [16] is used to describe the interface evolution in time numerically.

Let us now specify the boundary conditions for Eq. (2). We note that the value $x = L$ corresponds to the slowly and uniformly drying region of the film, which implies

$$h_x(L) = 0, \tag{4}$$

$$h_{xxx}(L) = 0. \tag{5}$$

Near $x = 0$, the solid surface is assumed "dry" from the macroscopic point of view, i.e., it is covered with a microscopic adsorbed film where the evaporative mass flux is suppressed by van der Waals forces. Thickness of this equilibrium film is found from the condition of zero mass flux across the interface. For nonpolar liquids, this condition gives

$$h_{af} = \left(\frac{\varepsilon\delta}{T_0}\right)^{1/3},$$

while for polar liquids h_{af} is found from the zero-flux condition numerically.

Since the film is flat at $x = 0$, all derivatives have to be zero. This was relatively easy to satisfy for steady contact

lines [12] when an ordinary differential equation for the interface profile was solved using a shooting method. However, for unsteady interface evolution considered in the present work the number of boundary conditions for the evolution equation is limited and so it is not clear *a priori* how to ensure that all derivatives are zero near $x=0$. A remarkable feature of the numerical solution illustrated below is that the miscroscopic film remains flat near $x=0$ when only two boundary conditions are specified in the form

$$h(0) = h_{af}, \quad h_x(0) = 0.$$

The initial condition is a discontinuous function equal to h_{af} for $[0, L/3]$ and equal to 1 on the remaining two thirds of the interval.

Let us first study liquid-vapor interface evolution in nonpolar liquids by running the simulation with $S=0$ in the expression for the disjoining pressure given by Eq. (3). After a very short transient period the solution becomes smooth and evolves further on relatively slow time scales. Snapshots of typical interface shapes are shown in Fig. 1(a) for $L=20$ and 600 mesh points; values of all nondimensional parameters are listed in the caption. Formation of the capillary ridge observed in experiments is clearly seen in the simulations as well. The interface deformation is localized near the dry area. Far away from it the film simply dries out by evaporation in a uniform fashion. We have chosen a relatively large value of ε to make the microscopic film visible, but the code has been tested for values of ε down to 10^{-6}. Such small and more physically realistic values of ε are used later in this article to simulate growth and interaction of circular dry patches. The values of the kinetic parameter K for water films are on the order of 10^{-2} or 10^{-3} under typical experimental conditions, the dimensional superheat that corresponds to $T_0=0.1$ is approximately 0.3 K. We note that the small values of nondimensional parameters, especially ε, impose severe limitations on the applicability of the lubrication-type approach used in the present study. However, this approach is known to produce results which are in good agreement with experiments and numerical simulations even outside the range of its formal asymptotic validity [15].

Details of the vapor-liquid interface shape are rarely investigated experimentally, while data for the time-dependent position of the contact line is easy to obtain. Therefore it is important to be able to record contact line position based on our simulations as well. Let us define the position of the contact line as the point of maximum curvature of the interface. This definition is appropriate since the contact line in our approach is a highly localized region of rapid change of interfacial slope. Typical results for contact line position versus time for a nonpolar liquid are shown in Fig. 1(b). The contact line speed increases slightly with time, which can be explained by a higher intensity of evaporation in films of smaller thickness at the late stages of dry-out.

Let us now consider polar liquids and use the appropriate form of the expression for the disjoining pressure, Eq. (3) with $S=1$ and $\xi=10.9$. Here we consider very thin films of water (in the range of thickness between 10 and 100 nm) and choose parameter values (listed in the caption) which are based on the dimensional values used in Ref. [8] to describe

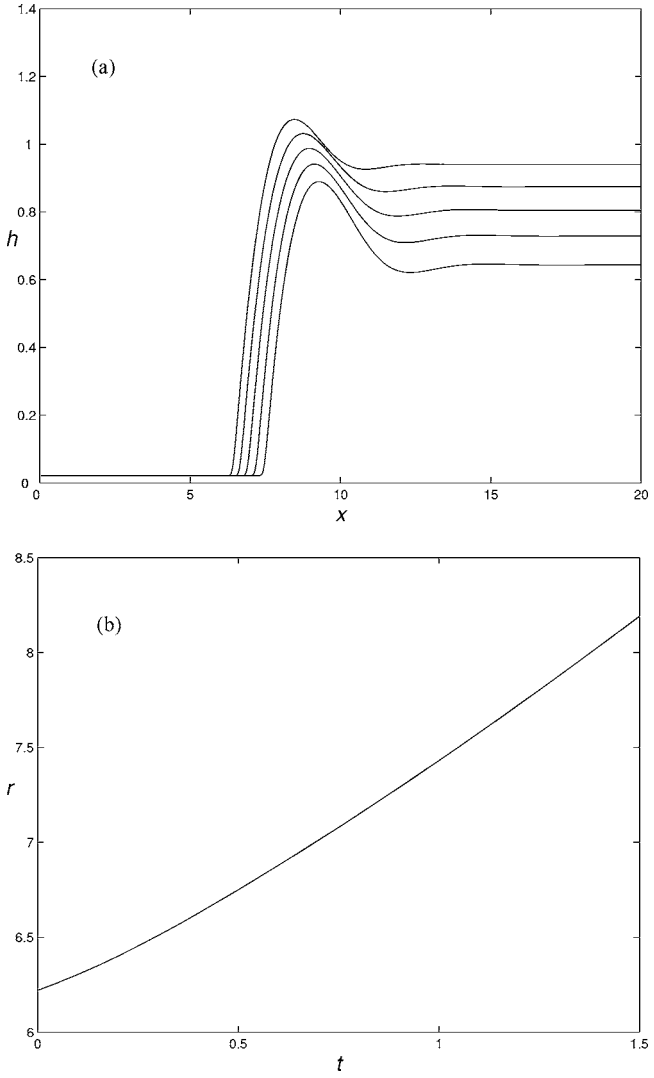

FIG. 1. Snapshots of the interface deformation (a) and position of contact line (b) for nonpolar liquids ($S=0$), $K=0.02$, $\delta=10^{-2}$, $\varepsilon=10^{-4}$, $T_0=0.1$, $M=0$.

experimental results on dry-out in polar liquids ($A=10^{-20}$ J, $d_0=0.2$ nm, $l_0=0.6$ nm). The initial condition is again a discontinuous function that jumps from the unit thickness to the adsorbed film value. Typical results are illustrated in Fig. 2. Initially the evolution is similar to the case of nonpolar liquids shown above: the thicker part of the film decreases its height by evaporation and a capillary ridge is formed ahead of the moving contact line. However, at the later stages of evolution, the presence of electrical double layer results in rapid decrease of the thinning rate of the film and significant decrease in the height of the capillary ridge. The latter in fact becomes almost impossible to observe. The motion of the contact line can then be described as propagation of a front between two different equilibrium values of film thickness, the contact line speed becomes essentially constant, in agreement with experimental observations of dry-out in polar liquids [3]. This regime has been studied by Lyushnin *et al.* [8] in the framework of a slightly different model of evaporating films. The contact line speed as a function of evaporation kinetic parameter K is shown in Fig. 3. Clearly, for higher

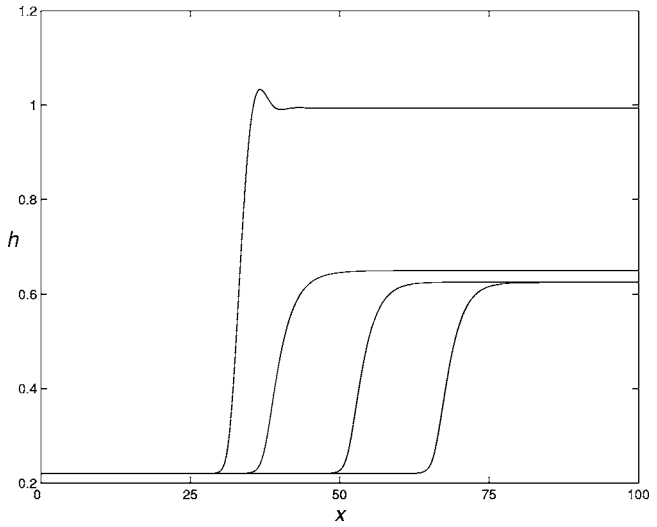

FIG. 2. Snapshots of the interface for polar liquid, $S=1$, $\delta=0.1$, $\varepsilon=10^{-2}$, $T_0=0.003$, $\xi=10.9$, $M=0$, $K=0.02$.

evaporation rate (lower K) the contact line speed is higher since evaporation is the driving force of the expansion of dry patches. The maximum speed is achieved when the kinetic effects at the interface are negligible ($K=0$).

Thermocapillary effect can have a significant influence on dewetting in evaporating films. Marangoni stresses are coupled to temperature field in the liquid, so they cannot be described in the framework of models that do not include heat transfer in the film. The present model is free from this limitation: the evolution equation (2) provides a consistent description of thermocapillary stresses in terms of the modified Marangoni number M. An interesting feature of the simulation results for nonzero M is that the effect of thermocapillarity on the contact line speed can be different depending on film thickness. For thicker films, the contact line speeds up due to Marangoni effect, while for thinner films thermocapillarity has the opposite effect. This is illustrated in Fig. 4 for $M=2$ (solid line), where both effects are captured

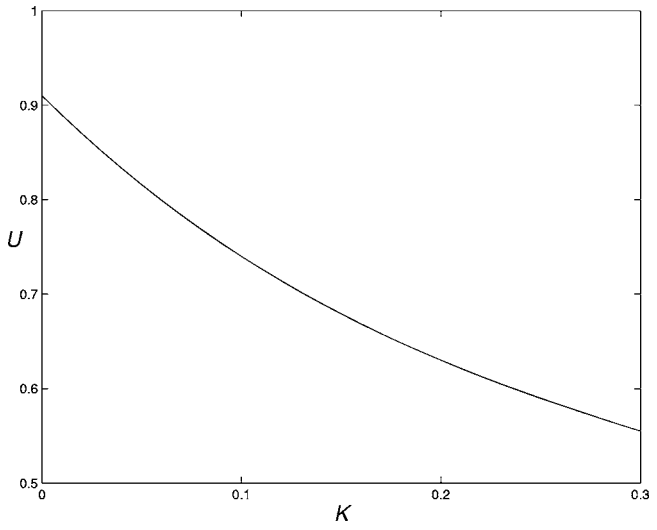

FIG. 3. Contact line speed as a function of kinetic parameter for polar liquids $S=1$, $\delta=0.1$, $\varepsilon=10^{-2}$, $T_0=0.003$, $\xi=10.9$.

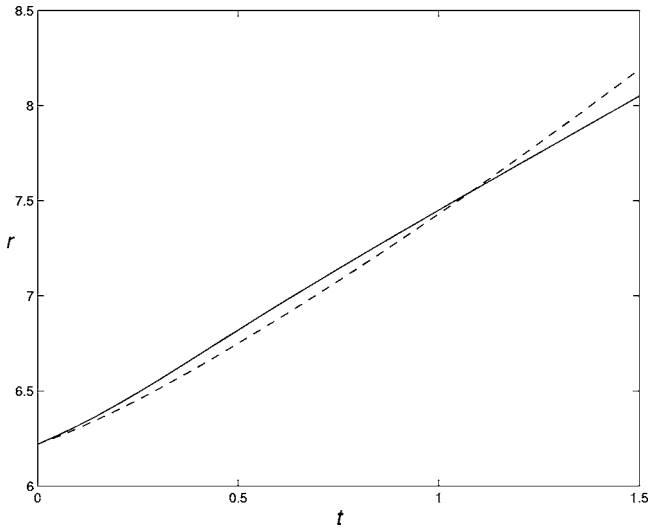

FIG. 4. The effect of Marangoni stresses on the contact line speed for $K=0.02$, $\delta=10^{-2}$, $S=0$, $\varepsilon=10^{-4}$, $T_0=0.1$. Position of contact line is shown for $M=2$ (solid line) and $M=0$ (dashed line).

at different stages of film evolution (dashed line corresponds to $M=0$). The speed-up of the contact line is not difficult to explain: it has to do with the fact that temperature near the contact line is higher and so Marangoni flow tends to speed up the removal of liquid. In order to understand the slowdown observed for thinner films, we investigated the interface shape for different values of M and observed that liquid tends to accumulate in the capillary ridge. This accumulation results in a significant reduction of the evaporation rate and thus slows down the contact line.

IV. FINGERING INSTABILITY

Fingering instabilities have been studied extensively for isothermal thin film flows driven by gravity. Experimental observations of a viscous flow down an inclined plane show that an initially straight contact line can become unstable, resulting in formation of fingers, i.e., liquid rivulets protruding towards the dry area [17]. Mathematical models that determine the criteria for such instability have been formulated using a lubrication-type framework [18].

When body forces are negligible but temperature in the film is nonuniform, the main physical effects that can affect contact line dynamics are thermocapillarity and evaporation. Careful investigations of the former were carried out and included results on both stability criteria and nonlinear evolution of the contact lines [19,20]. Evaporation has received much less attention even though experimental studies [3] indicate that fingering instabilities can develop in evaporating thin films. Lyushnin *et al.* [8] studied fingering instabilities in the model of growing dry patches in ultra-thin films and showed both analytically and numerically that evaporation can have a stabilizing effect on this instability. However, the model of Ref. [8] is limited to a relatively narrow range of physical parameters when the moving front between two steady ultrathin films is observed and is based on the assumption of negligible Marangoni stresses. In the present

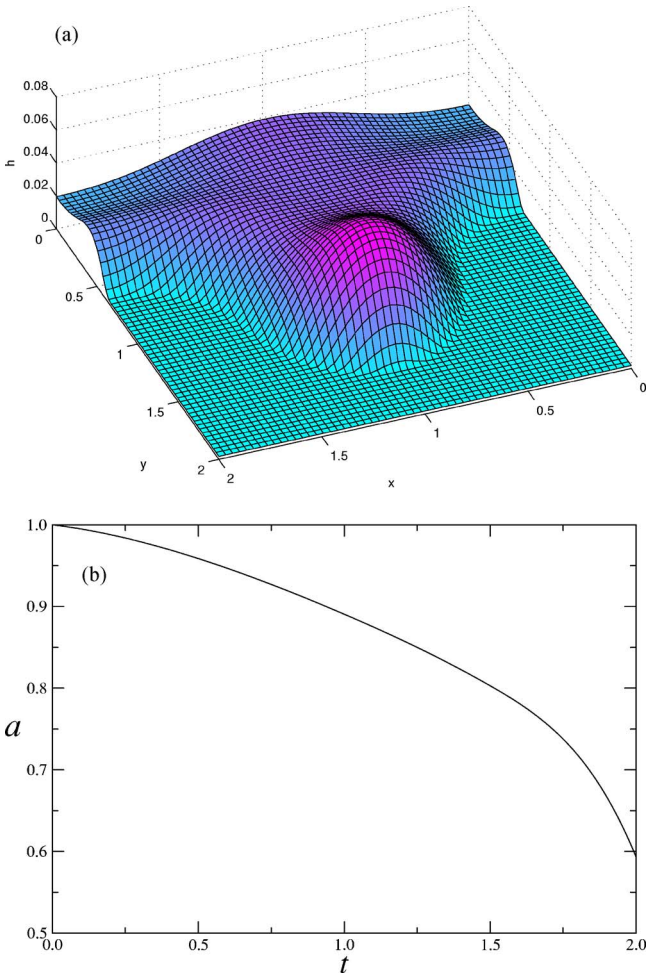

FIG. 5. (Color online) (a) Typical shape of a finger formed due to action of Marangoni stresses in the limit of weak evaporation. (b) The effect of evaporation on scaled perturbation amplitude for $\delta=10^{-2}$, $\varepsilon=10^{-4}$, $M=2$, $G=-1$, $S=0$, and $K^{-1}=0.01$.

study we use the model from Sec. II to study the combined effect of thermocapillarity and evaporation on fingering instabilities.

Let us first consider the case of large values of K which corresponds to negligible evaporation and choose the substrate temperature profile in the form

$$T_0 = T_{00} + Gy. \tag{6}$$

We discuss the instability in a two-dimensional framework suggested, e.g., in Ref. [8]. For a fixed value of $M=2$ and a range of L, we observe that small perturbations of initially straight contact line grow to form fingers, as illustrated in Fig. 5(a) (for the limiting case of $K^{-1}=0$). This behavior is similar to the dynamics observed by Sur *et al.* [20] in the framework of a slightly different model. When evaporative mass flux is included in the formulation, it acts to supress the instability. In order to describe this effect quantitatively, we introduce the difference between the largest and the smallest values of y along the contact line, scaled by its initial value. This quantity, denoted by a, is shown in Fig. 5(b) as a function of time for $K^{-1}=0.01$. Clearly, even for relatively weak evaporation the Marangoni-driven fingering instability is suppressed. When the Marangoni number is increased, the initial growth rate of instability also increases for the case of negligible evaporation, but for $K^{-1}=0.01$ the instability is still suppressed for a range of values of M.

The instability illustrated in Fig. 5(a) is most likely due to a capillary mechanism that has to do with formation of the capillary ridge ahead of the moving contact line. This mechanism is analogous to Rayleigh instability of liquid jets and cylinders. We note that in experiments the effect of surfactants may also be important as discussed, e.g., in Ref. [21].

V. DRY PATCHES IN THREE-DIMENSIONAL SIMULATIONS

Let us now study formation and interaction of dry patches using the full two-dimensional numerical solution of the differential equation (2) for film thickness. Significant potential of disjoining pressure models for such simulations has been demonstrated in the literature in the framework of simplified evaporation models [7]. In the simulations discussed below we assume the liquid to be nonpolar, i.e., we choose the expression for Π that includes only van der Waals forces, although similar results can be obtained for polar liquids. Computational domain is a square box of dimensions $L\times L$.

We start by considering a single dry patch. The initial condition for the simulation is chosen as an axisymmetric step function that jumps from an ultrathin film to a macroscopic film of uniform thickness. The interface shape becomes rather smooth on a very fast time scale and then propagates without changing its shape significantly. A typical snapshot of the dry patch is shown in Fig. 6(a). This dynamics is similar to that discussed in Sec. III. We note that the characteristic capillary ridge is formed ahead of the boundary of the expanding dry area. The rate of expansion can be recorded from the numerical simulation based on the position of the contact line. Since the contact line in our simulation is in fact a transition region associated with rapid change of curvature, there are several possible definitions of its position. We choose the point of maximum curvature as the definition of the contact line and plot its position in Fig. 6(b). The dependence is close to linear, but the growth rate of the dry patch increases with time slightly. This is an indication of the fact that the overall average film thickness decreases and thus evaporation becomes more intense. We note that this effect cannot be captured by the models that assume the front to be a transition zone between two regions of uniform thickness.

An important advantage of the description of contact line proposed in the present study is that it allows one to simulate topological changes in films with many dry areas of arbitrary shape without any special subroutines for tracking contact lines. In order to illustrate this we consider interaction and merger of dry patches into a single dry area. The results of simulations for the two patches are presented in Fig. 7. Snapshots of contact lines are shown at equal time intervals. As a result of interaction, both patches clearly change their shape. Initially, interaction slows down growth of each dry patch. This stage is followed by rapid acceleration of fronts towards

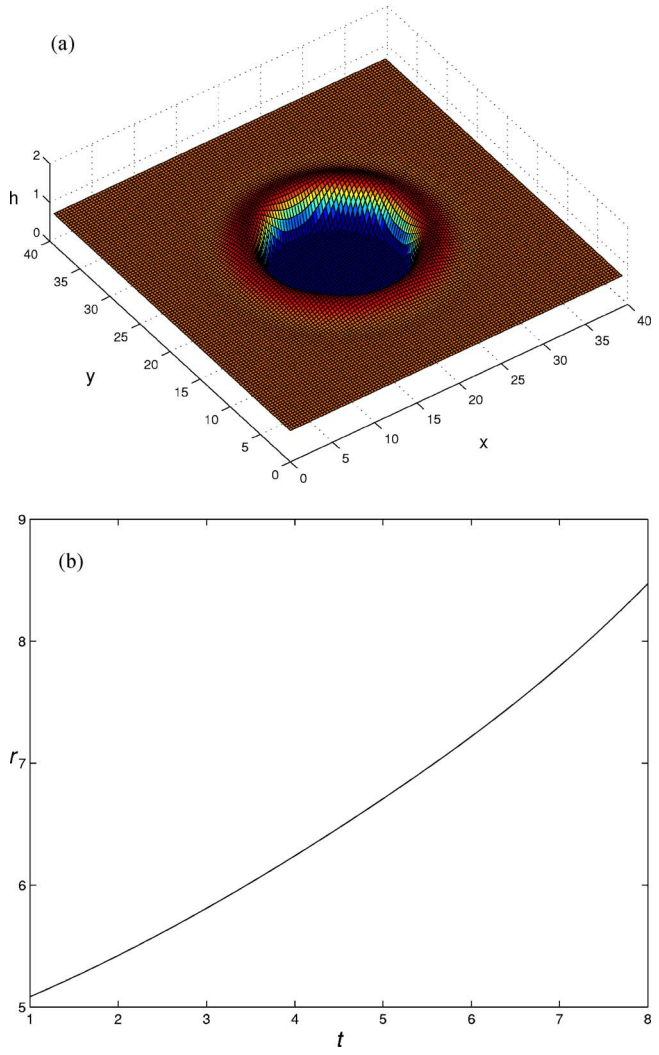

FIG. 6. (Color online) Typical interface shape (a) and dry patch radius as a function of time (b) for $K=0.01$, $\delta=10^{-3}$, $\varepsilon=10^{-6}$, $S=0$, $T_0=0.1$.

each other until the dry areas merge completely. This rapid dynamics can be explained by the decrease of the amount of liquid in the film between the patches.

We note that merger of the dry areas is easily handled by the code without any numerical difficulties, which clearly indicates the significant potential of the moving contact line model, developed in Ref. [13] and extended to polar liquids in the present work, for simulations of complicated wetting phenomena in evaporating liquid films. The present approach is somewhat analogous to phase field methods for simulations of moving interfaces. The contact line is represented as a region of rapid change of curvature and therefore topological changes are handled easily.

VI. CONCLUSIONS

Dewetting in evaporating liquid films is characterized by nucleation of localized macroscopically dry patches. Several investigations suggested that these dry areas are in fact covered by microscopic films that are in equilibrium with the vapor due to disjoining pressure. In the present work, this idea is incorporated in a carefully developed model of viscous flow, heat transfer, and evaporation in the film around growing dry patches. We demonstrate that the model can be used to describe complicated evolution of a two-dimensional interface in three-dimensional space and is capable of handling topological changes in the system, e.g., merger of two dry patches.

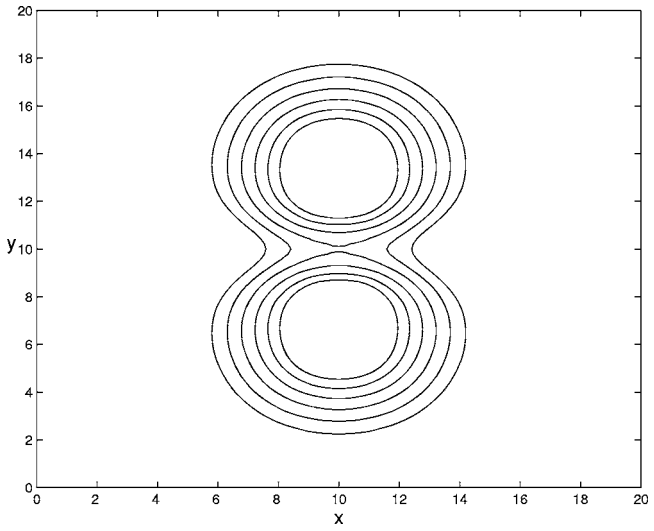

FIG. 7. Snapshots of contact line obtained from simulations of two-dimensional surface of evaporating liquid taken at equal time intervals separated by $\Delta t=1$ for $K=0.01$, $\delta=10^{-3}$, $\varepsilon=10^{-6}$, $T_0=0.1$.

For an isolated patch growing from an initially small dry area in otherwise uniform evaporating film we have recorded the contact line position as a function of time. We have found two different scenarios for growth of dry patches. For nonpolar liquids, the equilibrium microscopic film is formed due to van der Waals forces and contact line speed slightly increases with time as the dry patch grows. For polar liquids the equilibrium in the adsorbed film is due to a combination of van der Waals forces and formation of electrical double layers, contact line speed quickly approaches a constant value.

Simulations indicate that a capillary ridge is formed ahead of a growing dry patch. The ridge is more well defined for nonpolar liquids and provides a physical mechanism for an instability of the moving contact line which is indeed observed for a range of parameter values. The result of the instability is formation of fingers, i.e., liquid rivulets protruding toward the dry region. Thermocapillary forces are shown to increase the height of the capillary ridge and decrease the expansion rate of the dry patch if the film is sufficiently thin. For thicker films, Marangoni stresses tend to speed up expansion since they assist in removal of liquid from the regions near the dry area. Studies of two interacting dry patches indicate that at high separation distances the patches slow each other down, while rapid dynamics is observed as they come closer and finally merge.

ACKNOWLEDGMENTS

This work was supported by the National Science Foundation.

[1] E. B. Dussan, Annu. Rev. Fluid Mech. **11**, 371 (1979).
[2] P. G. de Gennes, Rev. Mod. Phys. **57**, 827 (1985).
[3] M. Elbaum and S. G. Lipson, Phys. Rev. Lett. **72**, 3562 (1994).
[4] S. Herminghaus, K. Jacobs, K. Mecke, J. Bischof, A. Fery, M. Ibn-Elhaj, and S. Schlagowski, Science **282**, 916 (1998).
[5] A. Sharma, Langmuir **14**, 4915 (1998).
[6] A. Oron and S. G. Bankoff, J. Colloid Interface Sci. **218**, 152 (1999).
[7] L. W. Schwartz, R. V. Roy, R. E. Eley, and S. Petrash, J. Colloid Interface Sci. **354**, 363 (2001).
[8] A. V. Lyushnin, A. A. Golovin, and L. M. Pismen, Phys. Rev. E **65**, 021602 (2002).
[9] M. Potash and P. C. Wayner, Jr., Int. J. Heat Mass Transfer **15**, 1851 (1972).
[10] S. Moosman and G. M. Homsy, J. Colloid Interface Sci. **73**, 212 (1980).
[11] S. DasGupta, J. A. Schonberg, I. Y. Kim, and P. C. Wayner, J. Colloid Interface Sci. **157**, 332 (1993).
[12] V. S. Ajaev and G. M. Homsy, J. Colloid Interface Sci. **240**, 259 (2001).
[13] V. S. Ajaev, J. Fluid Mech. **528**, 279 (2005).
[14] J. P. Burelbach, S. G. Bankoff, and S. H. Davis, J. Fluid Mech. **195**, 463 (1988).
[15] A. Oron, S. G. Bankoff, and S. H. Davis, Rev. Mod. Phys. **69**, 931 (1997).
[16] P. N. Brown, C. D. Byrne, and A. Hindmarsh, SIAM (Soc. Ind. Appl. Math.) J. Sci. Stat. Comput. **10**, 1038 (1989).
[17] H. E. Huppert, Nature (London) **300**, 427 (1982).
[18] A. L. Bertozzi and M. P. Brenner, Phys. Fluids **9**, 530 (1997).
[19] A. M. Cazabat, F. Heslot, S. M. Troian, and P. Carles, Nature (London) **346**, 824 (1990).
[20] J. Sur, T. P. Witelski, and R. P. Behringer, Phys. Rev. Lett. **93**, 247803 (2004).
[21] O. K. Matar and S. M. Troian, Phys. Fluids **11**, 3232 (1999).